

Atmospheric Flash Drought in the Caribbean

CRAIG A. RAMSEYER^a AND PAUL W. MILLER^b

^a *Department of Geography, Virginia Polytechnic Institute and State University, Blacksburg, Virginia*

^b *Department of Oceanography and Coastal Sciences, Louisiana State University, Baton Rouge, Louisiana*

(Manuscript received 28 November 2022, in final form 24 July 2023, accepted 6 September 2023)

ABSTRACT: Despite the intensifying interest in flash drought both within the United States and globally, moist tropical landscapes have largely escaped the attention of the flash drought community. Because these ecozones are acclimated to receiving regular, near-daily precipitation, they are especially vulnerable to rapid-drying events. This is particularly true within the Caribbean Sea basin where numerous small islands lack the surface and groundwater resources to cope with swiftly developing drought conditions. This study fills the tropical flash drought gap by examining the pervasiveness of flash drought across the pan-Caribbean region using a recently proposed criterion based on the evaporative demand drought index (EDDI). The EDDI identifies 46 instances of widespread flash drought “outbreaks” in which significant fractions of the pan-Caribbean encounter rapid drying over 15 days and then maintain this condition for another 15 days. Moreover, a self-organizing maps (SOM) classification reveals a tendency for flash drought to assume recurring typologies concentrated in one of the Central American, South American, or Greater Antilles coastlines, although a simultaneous, Caribbean-wide drought is never observed within the 40-yr (1981–2020) period examined. Furthermore, three of the six flash drought typologies identified by the SOM initiate most often during Phase 2 of the Madden–Julian oscillation. Collectively, these findings motivate the need to more critically examine the transferability of flash drought definitions into the global tropics, particularly for small water-vulnerable islands where even island-wide flash droughts may only occupy a few pixels in most reanalysis datasets.

SIGNIFICANCE STATEMENT: The purpose of this study is to understand if flash drought occurs in tropical environments, specifically the Caribbean. Flash droughts represent a quickly evolving drought, which have particularly acute impacts on agriculture and often catch stakeholders by surprise as conditions evolve rapidly from wet to dry conditions. Our results indicate that flash droughts occur with regular periodicity in the Caribbean. Expansive flash droughts tend to occur in coherent subregional clusters. Future studies will further investigate the drivers of these flash droughts to create early warning systems for flash drought.


KEYWORDS: Tropics; Drought; Extreme events; Climate

1. Introduction

Flash drought has recently gained momentum as a paradigm to describe rapid-onset drought events that develop due to the superposition of both high evaporative demand and insufficient rainfall (Vicente-Serrano et al. 2010; Beguería et al. 2014). While rapid-onset droughts have been observed over the U.S. Central Plains in 2012, 2016, and 2017 (Otkin et al. 2018), conventional drought definitions based on months-long precipitation anomalies (e.g., McKee et al. 1993) can either miss these events altogether, underestimate their severity, and/or truncate the length of the dry period following the rapid onset. Given these shortcomings, several methods of flash drought identification have been proposed that each attempt to capture instances of rapid landscape desiccation (e.g., Osman et al. 2021). For instance, Ford and Labosier (2017) suggested a transition in 0–40-cm volumetric water content from above the 40th to below the 20th percentile within four 5-day pentads,

whereas Yuan et al. (2019) amended their definition to require at least a minimum of 5-percentile declines in root zone soil moisture per pentad. Meanwhile, Mo and Lettenmaier (2015) explicitly attached temperature and evapotranspiration (ET) requirements to the soil moisture criterion in an attempt to identify “heat wave flash droughts,” which they viewed as distinct from precipitation-driven flash droughts (Mo and Lettenmaier 2016). Otkin et al. (2018) added additional nuance to the flash drought paradigm by distinguishing agricultural and ecological flash droughts from other drought contexts (i.e., meteorological or hydrological). Beyond soil moisture, temperature, and ET anomalies, Hobbins et al. (2016) introduced a new metric derived from a statistical transformation of reference evapotranspiration, called the evaporative demand drought index (EDDI).

Regardless of metric or definition, one theme that unites nearly all flash drought analyses is a midlatitude study area. For instance, the semiarid landscape of the U.S. Great Plains, where comparatively sparse vegetation can succumb to heat anomalies and wilting rather quickly, has motivated many flash drought studies. However, midlatitude biomes are also accustomed to multiday dry spells that can sometimes persist for months. For instance, Dallas, Texas, has experienced 56 dry spells of ≥ 21 days between 1991 and 2020, whereas San Juan,

 Denotes content that is immediately available upon publication as open access.

Corresponding author: Craig A. Ramseyer, ramseyer@vt.edu

DOI: 10.1175/JHM-D-22-0226.1

© 2023 American Meteorological Society. This published article is licensed under the terms of the default AMS reuse license. For information regarding reuse of this content and general copyright information, consult the AMS Copyright Policy (www.ametsoc.org/PUBSReuseLicenses).

Brought to you by NOAA Central Library | Unauthenticated | Downloaded 01/16/24 09:02 PM UTC

TABLE 1. Comparison of number of dry spells (consecutive days of precipitation < 0.25 mm) between 1991 and 2020 that were greater than or equal to 14, 7, and 3 days in duration at four locations in the U.S. Great Plains vs one in the neotropics. Frequencies were retrieved from xMACIS2 (<https://xmacis.rcc-acis.org/>).

Location	14 days	7 days	3 days
Denver, CO (KDEN)	137	468	972
Omaha, NE (KOMA)	77	363	1039
Wichita, KS (KICT)	117	445	967
Dallas, TX (KDFW)	133	451	944
San Juan, PR (KSJU)	8	108	600

Puerto Rico, has only experienced two such events. While not a flash-drought criterion, Table 1 shows that this same pattern exists across multiple dry-spell lengths and continental locations, with the midlatitude-versus-wet-tropical disparity becoming more apparent at longer durations. In addition to encountering regular, moderate precipitation, wet tropical climates experience high relative humidity year-round, and relatively low temperature variability. Thus, the typical flash drought conceptualization of little rain and high ET demand during exceptional heat waves is of dubious relevance to wet tropical biomes.

Nonetheless, moist tropical ecosystems can and do experience rapid-onset drying accompanied by the swift accumulation of biological consequences. For instance, during the onset of the historic 2015 Caribbean drought, soil O₂ concentrations in Puerto Rico's Luquillo Mountains increased from 5.6% to 11.2% in one week during late April while soil moistures experienced a 63% decline during a 21-day period extending into early May (O'Connell et al. 2018). Litterfall collected in the Luquillo Mountains hit a sharp peak in mid-May 2015 that was 3.5 times the May average during the previous 12 years (Zimmerman et al. 2016). Elsewhere, epiphytes in moist tropical settings can completely dry out after as little as three days without rain (Köhler et al. 2007). Because these ecosystems are so highly adapted toward regular moderate precipitation with relatively stable temperature regimes, even small warming events coupled with week-long dry spells may constitute ecological "flash drought" in these landscapes. Thus, the prompt diagnosis of incipient flash drought is imperative for wet tropical environments. Fortunately, Gingrich (2022) found that the aforementioned EDDI generated a realistic sequence of flash drought in Puerto Rico that corresponded with several known rapid drying events that coincided with ecological stress in the Puerto Rico's Luquillo Mountains.

Consequently, this study will investigate the transferability of the EDDI as well as its associated flash drought definition in Pendergrass et al. (2020) to wet tropical landscapes across the entire Caribbean basin. The primary objectives of this study are to: 1) Characterize the patterns of EDDI observed in the Caribbean Sea region; 2) Evaluate the spatial distribution and variability of flash drought across the Caribbean using EDDI and machine learning classification techniques; and 3) Investigate the relationship between Caribbean flash drought frequency and subseasonal modes of climate variability.

2. Data and methods

a. ERA5-Land

This study uses the newly released ERA5-Land reanalysis dataset to calculate EDDI on the native grid. By using this new gridded dataset, a high-resolution spatiotemporal analysis of flash drought can be performed across the entire Caribbean region, no longer being constrained to coarser gridded datasets and/or the sparsely distributed long-term observation datasets in the region. While ERA5-Land reanalysis still has limitations for our context, such as lack of soil moisture observations for many small Caribbean islands, this dataset allows for new insight into better understanding the spatial distribution and patterns of drought (Muñoz-Sabater et al. 2021).

ERA5-Land outputs 50 variables over land, globally, hourly, and at a 9-km spatial resolution, aligning with the ECMWF triangular-cubic-octahedral operational grid (Malardel et al. 2016). ERA5-Land is available from 1950 to the present; however, this study will focus on 1981–2020 as it ensures adequate satellite data are used in the ERA5 data assimilation and translates to higher confidence and accuracy (Hersbach et al. 2020). For a comprehensive overview of ERA-Land, see Muñoz-Sabater et al. (2021).

ERA5-Land provides the incoming radiative, temperature, moisture, and wind data for the derivation of ASCE reference ET and EDDI. These data were acquired every 1 h for the years 1981–2020. The back-extension ERA5-Land dataset is not used here because of its lack of satellite data in the data assimilation scheme, which causes the reanalysis to be heavily driven by the underlying model and in situ observations, of which there are very few in the study domain.

b. EDDI

EDDI is a drought index formulated to assess the atmospheric evaporative demand. Formally, this allows for a quantitative estimate of the "thirst" of the atmosphere. Following the methodology of Hobbins et al. (2016) to derive EDDI, we first calculate the standardized reference ET, or E_0 , which is a measure of atmospheric evaporative demand and is the rate at which readily available soil water is vaporized from specified vegetated surfaces (Jensen et al. 1990). The reference surface is normally mathematically expressed as a hypothetical vegetated surface with specific characteristics normally determined by the crop height (Allen et al. 1998). To leverage the highest temporal resolution estimates available from ERA5-Land, the reference ET is calculated exactly following the hourly ASCE Standardized Reference Evapotranspiration Equation for short reference crops (Allen et al. 2005):

$$E_0 = \frac{0.408\Delta(R_n - G) + y \frac{C_n}{T_{\text{air}} + 273} U(e_{\text{sat}} - e_a)}{\Delta + y(1 + C_d U)}, \quad (1)$$

where E_0 is hourly standardized reference ET, Δ (kPa °C⁻¹) is the slope of the saturated vapor pressure–temperature curve at the 2-m air temperature (°C), y (kPa °C⁻¹) is the psychrometric constant, U (m s⁻¹) is the wind speed (here specified at a 2-m height), R_n (MJ m⁻² h⁻¹) is the net radiation at the crop surface, G (MJ m⁻² h⁻¹) is the soil heat flux density, T_{air} is the mean

hourly air temperature ($^{\circ}\text{C}$), e_{sat} (Pa) and e_a (Pa) are the hourly saturated and actual vapor pressures, and C_n ($\text{K mm s}^3 \text{ Mg}^{-1} \text{ h}^{-1}$) and C_d (s m^{-1}) are respectively the hourly numerator and denominator constants for the short crop reference.

The hourly calculations of reference ET require sun angle information to determine if the ET calculation is occurring during daytime or nighttime, as determined by the hourly R_n value (e.g., $R_n > 0$ are considered daytime). Additionally, there are variables embedded in the R_n calculation that also require sun angle information, particularly the cloudiness function in the net outgoing long-wave radiation calculation. The cloudiness function chosen was dependent on if the sun angle at the midpoint of the hour was greater or less than 0.3 radians ($\sim 17^{\circ}$) following (Allen et al. 2005).

Hourly G , C_n , and C_d for standardized short reference ET are determined by

$$G_{\text{hr,daytime}} = 0.1R_n, \quad (2)$$

$$G_{\text{hr,nighttime}} = 0.5R_n, \quad (3)$$

$$C_{n,\text{daytime}} = 37, \quad (4)$$

$$C_{n,\text{nighttime}} = 37, \quad (5)$$

$$C_{d,\text{daytime}} = 0.24, \quad \text{and} \quad (6)$$

$$C_{d,\text{nighttime}} = 0.96. \quad (7)$$

Readers are encouraged to read the hourly time-step section of (Allen et al. 2005) for full details on the full hourly reference ET calculation.

Upon calculating hourly E_0 at all of the ERA5-Land grid points in the study domain, pentad (5-day mean) E_0 were derived. In the tropics, the radiation terms in Eq. (1) are larger magnitudes than those measured in the midlatitudes. As such, we aggregate hourly E_0 to the pentad-scale instead of the weekly scale E_0 used in Hobbins et al. (2016). Additionally, drying on the daily time scale can be impactful to other physical and biological systems in several locations in the study domain, such as the Luquillo Mountains in northeast Puerto Rico where biogeochemical systems have been shown to respond to drying on intra-weekly time scales (O'Connell et al. 2018). After pentad E_0 is derived, the nonparametric EDDI can be calculated following Hobbins et al. (2016) by first calculating the Tukey plotting position (Wilks 2011) that contextualizes the pentad E_0 values in the climatological distribution for a period of interest, in this study, pentads:

$$P(E_0) = \frac{i - 0.33}{n + 0.33}, \quad (8)$$

where $P(E_0)$ is the pentad empirical probability of E_0 for each pentad in the calendar year (leap days removed); i is the rank of the pentad E_0 in the time series from 1981 to 2020; and n is the number of observed pentads in the series being ranked, in this study n is 40 (total number of years in study period). For example, all 1–5 January E_0 values in the 40-yr dataset are

compared with one another to determine the rank of each pentad.

The final EDDI is calculated using an inverse normal approximation following Vicente-Serrano et al. (2010) and Hobbins et al. (2016):

$$\text{EDDI} = W - \frac{C_0 + C_1 W + C_2 W^2}{1 + d_1 W + d_2 W^2 + d_3 W^3}. \quad (9)$$

The following are defined constants: $C_0 = 2.515517$, $C_1 = 0.802853$, $C_2 = 0.010328$, $d_1 = 1.432788$, $d_2 = 0.189269$, and $d_3 = 0.001308$. The W term is dependent on the value of $P(E_0)$ from Eq. (8). If $P(E_0) \geq 0.5$, then $W = \sqrt{-2 \ln[P(E_0)]}$, else $W = \sqrt{-2 \ln[1 - P(E_0)]}$ and the sign of EDDI needs to be reversed. The resulting EDDI value is scaled in a minus/plus range that is a function of n and a value of 0 represents the median for that pentad. Positive EDDI values represent higher than normal evaporative demand, and thus, drier-than-normal conditions, whereas negative EDDI values represent lower than normal evaporative demand and wetter conditions. More details regarding the EDDI derivation can be found in Hobbins et al. (2016).

c. Self-organizing maps

Self-organizing maps (SOMs) are used in this study to explore the spatial patterns of EDDI and flash drought in the Caribbean. SOMs are commonly used in the field of synoptic climatology (e.g., Hewitson and Crane 2002; Sheridan and Lee 2011; Cassano et al. 2015; Mattingly et al. 2016; Teale and Robinson 2020; Ramseyer and Teale 2021) with several previous applications to hydroclimatology in the Caribbean (Ramseyer and Mote 2016, 2018; Ramseyer et al. 2019). SOMs are an implementation of machine learning (i.e., neural network) that is tuned for pattern recognition. Specifically, during model training, SOMs place vectors in the data space (i.e., nodes) that iteratively update to minimize error between the node vectors and all of the input vectors (e.g., Hewitson and Crane 2002; Sheridan and Lee 2011). For climatological research, SOMs have a distinct advantage over other dimensionality-reduction methods (e.g., principal component analysis) in that SOMs preserve all of the input data. As such, every input vector (i.e., each spatialized pentad of EDDI) gets mapped to the closest node vector. This allows for compositing of all input data that are mapped to each respective node. The training of the SOMs was completed using the SOM Toolbox, version 2.1 (Vesanto et al. 2000). The final SOMs were created using sequential training for 1000 iterations and were initialized on a lattice-node structure. The lattice node structure follows best practices of SOM training, as lattice-structures ensure that adjacent nodes are equidistant from one another, which is not achieved using rectangular node structures (Vesanto et al. 2000).

In this study, two SOMs are presented. The first SOM uses ERA5-Land derived EDDI pentads as input vectors to resolve the spatial patterns of EDDI across the Caribbean. The second SOM is trained only using large flash drought events that occurred simultaneously at more than 125 grid points in an attempt to isolate flash droughts that were likely forced by

meso-to-synoptic-scale meteorological and climatological forcings. Flash droughts that occur at fewer than 125 grid points concurrently include flash droughts that could be driven by more localized forcings and are harder to classify into recurring pan-Caribbean typologies using the SOM. While these events may be the focus of future work, those events are not included in this analysis.

d. Flash drought definition

This study utilizes an experimental EDDI-derived flash drought definition, proposed by Pendergrass et al. (2020), which recommends using percentile changes in EDDI in regions where the U.S. Drought Monitor is unavailable. As all areas in the study domain except Puerto Rico and the U.S. Virgin Islands are not analyzed in the U.S. Drought Monitor, we opt for the EDDI approach detailed below. Additionally, the U.S. Drought Monitor has only been fully operationalized in the U.S. Virgin Islands in the last 5 years, thus limiting its use in climatological studies.

Flash droughts are defined in this study by examining 30-day trajectories of EDDI at all land grid points in the study domain, which includes the Greater and Lesser Antilles as well as the Caribbean coastlines of Central and South America. Similarly, to Pendergrass et al. (2020), a flash drought occurs in this study when the pentad-mean EDDI has a 50-percentile increase over 3 pentads (15 days) and is maintained for the following 3 pentads (15 days). The advantages of this approach for the present study are twofold. First, the approach utilizes EDDI, which can be calculated only using atmospheric variables. This is important in this study domain due to a lack of long-term soil moisture sensors in the study domain. The low density of soil moisture observations for data assimilation, particularly in the early part of our study period, may limit the efficacy of soil moisture reanalysis data. Second, this approach is more transferable to eventual operational flash drought detection in numerical weather prediction model forecasts.

To illustrate this idea, Fig. 1 provides an analysis of ERA5-Land soil moisture (brown) and EDDI (green) during flash droughts ($n = 39\,900$ across all grid points). Figure 1 shows the comparative delay in the soil moisture response, whereas EDDI becomes positive two pentads before negative soil moisture anomalies are detected (Mukherjee and Mishra 2022). Thus, EDDI may provide ~10-day lead time on negative soil moisture anomalies as it pertains to flash droughts in the Caribbean.

e. Madden-Julian oscillation phases

The Madden-Julian oscillation (MJO) is one of the leading modes in subseasonal climate variability and has been widely applied in forecasting methods along the seasonal-to-subseasonal continuum (Madden and Julian 1972, 1994; Zhang 2005). Because flash drought is conceptualized to develop acutely on weeks-long time scales, the MJO is a logical forcing mechanism to consider in this context, and thus, an objective of this study is to identify potential relationships between the MJO and Caribbean flash drought frequency. The MJO is described according to eight integer-labeled phases, with each phase corresponding to a zonal region occupied by the cluster of clouds and rainfall

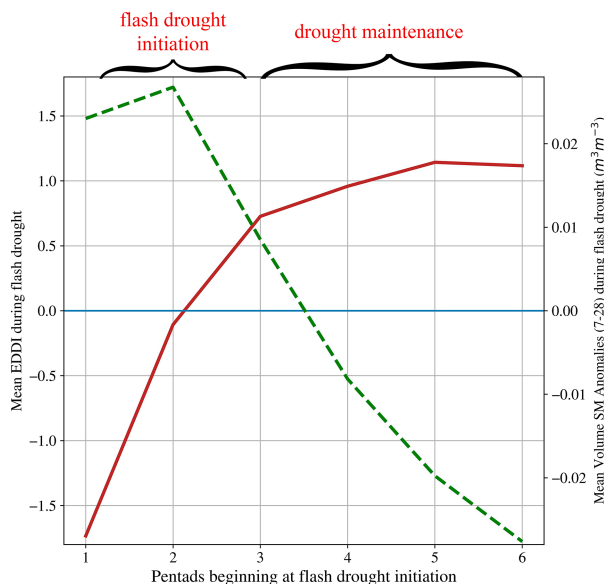


FIG. 1. Composite evolution of EDDI (solid red line) and soil moisture anomalies (7–28 cm; dashed green line) from all flash droughts at all ERA5-Land grid points ($n = 39\,900$).

marking the MJO's location. Additionally, the MJO phase must possess a minimum “amplitude” in order for its phase to be confidently determined (Wheeler and Hendon 2004). Daily MJO phases and amplitudes for the period of study were retrieved from the Australian Bureau of Meteorology (<http://www.bom.gov.au/climate/mjo/>). Only flash droughts that occur during MJO active phases (i.e., amplitude > 1.0) are considered in the analysis (e.g., Debbage et al. 2017).

The abrupt shift in EDDI required to meet flash drought definition (e.g., Fig. 1) is likely driven by an abrupt shift in broad atmospheric dynamics. To assess whether the MJO exhibits a nonrandom distribution during these flash drought events, a chi-square test is employed. The chi-square tests the null hypothesis that the MJO data are randomly and equally distributed during flash drought events in the Caribbean. This analysis is conducted on three temporal periods, a preinitiation, initiation, and maintenance period. Although the “flash” descriptor uniquely references the onset of the drought, mechanisms behind drought maintenance and length are nonetheless valuable for some stakeholder interests (Mercado-Díaz et al. 2023). The preinitiation and maintenance periods are 10 days (2 pentads) in length, while the initiation period the pentad where initiation occurred and designed to indicate if MJO phases are equally distributed across each of the temporal periods. The p values of the chi-square test are calculated to determine if the null hypothesis can be rejected at the 95% confidence level, in which case, the observed frequencies of MJO phases are not equally likely and implies that there is a link between MJO phase and flash drought initiation that motivates additional research on MJO and flash drought in the Caribbean.

Furthermore, the Climate Hazards Group InfraRed Precipitation with Station, version 2, data (CHIRPS2; Funk et al. 2015) are

used to assess pan-Caribbean precipitation patterns during each MJO phase. CHIRPS2 is a near-global 0.05° -resolution gridded rainfall product available from 1981 to the present (Funk et al. 2015). The mean daily rainfall for all days with an MJO amplitude of ≥ 1 is computed and then used to derive a phase-specific anomaly for each of the eight MJO phases. These anomaly maps are used to understand how the MJO trajectories associated with each flash drought typology identified by the SOM are tied to basin-wide precipitation patterns.

3. Results

a. EDDI SOMs

The spatial patterns of EDDI elucidated by a 15-node SOM are presented in Fig. 2. The most obvious similarity across all nodes is the large intra-regional variability in EDDI. While some nodes are nonetheless characterized by more pervasive wet or dry conditions than others, there are only two nodes (1 and 15) that characterize by a “consensus” hydroclimate condition. Otherwise, there is a large variability in the intra-Caribbean EDDI patterns. For instance, in nodes 3 and 6 the Central American coast experiences positive EDDI values, while the Greater Antilles typically encounter negative EDDIs. Similarly, nodes 7 and 14 are effective inverses of each other with Cuba demonstrating an opposite condition to the rest of the Caribbean in each case. While it is tempting to refer to “the Caribbean” as a monolithic hydroclimate region, Fig. 2 highlights that while large areas of the basin may experience a dominant wet or dry state, this condition is not universal.

Nonetheless, despite these being the composites of a large number of pentads, there are a few periods in the climatology for which a large portion of the Caribbean experiences positive EDDI values simultaneously (i.e., above-normal evaporative demand and drying). In particular, node 15 shows large EDDI values throughout the study area as with node 11, except for the highest elevations of Honduras and Nicaragua. Conversely, there are similar spatial patterns elucidated by the SOM across the study domain for low EDDI (wet conditions, lower evaporative demand), particularly in nodes 1–4. However, even within these largely dry or largely wet nodes, pockets of opposite moisture conditions are apparent. Even within node 4, which is characterized by some of the lowest EDDI (i.e., below-normal evaporative demand) values across the entire SOM, a region of positive EDDI occupies Cuba.

Unsurprisingly, given the thermodynamic forcing in the reference ET equation, most of the low EDDI nodes in the top-row of Fig. 2 have exhibited a statistically significant decreasing trend over the study period. Those trends are physically consistent as the bottom-row of the SOM, where the highest EDDI nodes have exhibited a statistically significant increasing trend over the study period.

Because the insular Caribbean is a water-vulnerable landscape and susceptible to drought, a nested SOM is produced to better understand the “flavors” of the basin’s most pervasive dry conditions. This nested SOM methodology involves creating a second SOM using only those pentads that map to node 15 in Fig. 2 (Ramseyer et al. 2022) because it represents the most

widespread high-EDDI pattern. The resulting 2×4 SOM shows the continuum of high-impact drying across the study region (Fig. 3). Because of the reduced sample size, a smaller number of nodes is selected to avoid nodes with very small numbers of samples. This nested SOM provides additional nuance in understanding the spatial variability of drying in the Caribbean. Node 1 of the nested SOM, which exhibits a statistically significant increasing trend over the study period, depicts a relatively universal high-EDDI condition, while Node 2 shows the most intense drying in the central part of the domain, including the Dominican Republic, Puerto Rico, and the U.S. Virgin Islands. In contrast, nodes 6–8 show pronounced drying in the southern part of the domain, that tapers off moving south-to-north, culminating with neutral or negative EDDI (or wet anomalies) in Cuba and Hispaniola. This suggests that the highest magnitude drying is often isolated to portions of the study domain and likely responds to a combination of synoptic and nuanced, localized atmospheric forcings.

b. Flash drought climatology

Applying the flash drought criteria to the EDDI analyses, the frequency and distribution of flash droughts across the pan-Caribbean region can be characterized. Because the regional patterns of EDDI suggest a spatial coherence to flash drought frequency, several basic climate analyses were performed at each grid point. Figure 4 shows the return interval of flash drought in the Caribbean with a large portion of the Caribbean experiencing flash drought at least once a decade. The complex topography of the insular Caribbean as well as the Central and South American coasts can yield tight juxtapositions of large versus small return intervals, which is likely related to ERA5-Land’s diminished performance in areas of high intra-gridcell landscape variability. In these settings, the slope of the topography as well as orographic cloud formation (Miller et al. 2018) may perturb the net incoming shortwave and longwave radiation terms used to calculate the EDDI. Regardless, these results show that flash droughts are a recurring phenomenon across much of the Caribbean basin. Given the 40-yr study period, areas with the shortest return intervals (3–4 years) experienced 10–13 flash droughts whereas areas with the longest return intervals (9+ years) experienced ~ 4 such events.

While most of the Caribbean experiences a dry season, normally from December–March (Miller et al. 2019), flash droughts are not confined to this period and can occur throughout the year. Figure 5 displays the spatial variability in the months associated with the greatest number of flash droughts based on the 40-yr analysis. As with the EDDI patterns in Fig. 2, there is intra-Caribbean variability in the most frequent flash drought months. For instance, the South American Caribbean and Hispaniola most frequently encounter flash droughts in the climatological dry season (e.g., December–March). Farther west, most of Cuba and Honduras experience flash drought most often during summer. As with Fig. 2, Fig. 5 highlights the need for caution when referring to the Caribbean as a monolithic hydroclimate region and reveals subbasin nuances to rapid drying patterns that are often absent in scientific literature. Furthermore, it is

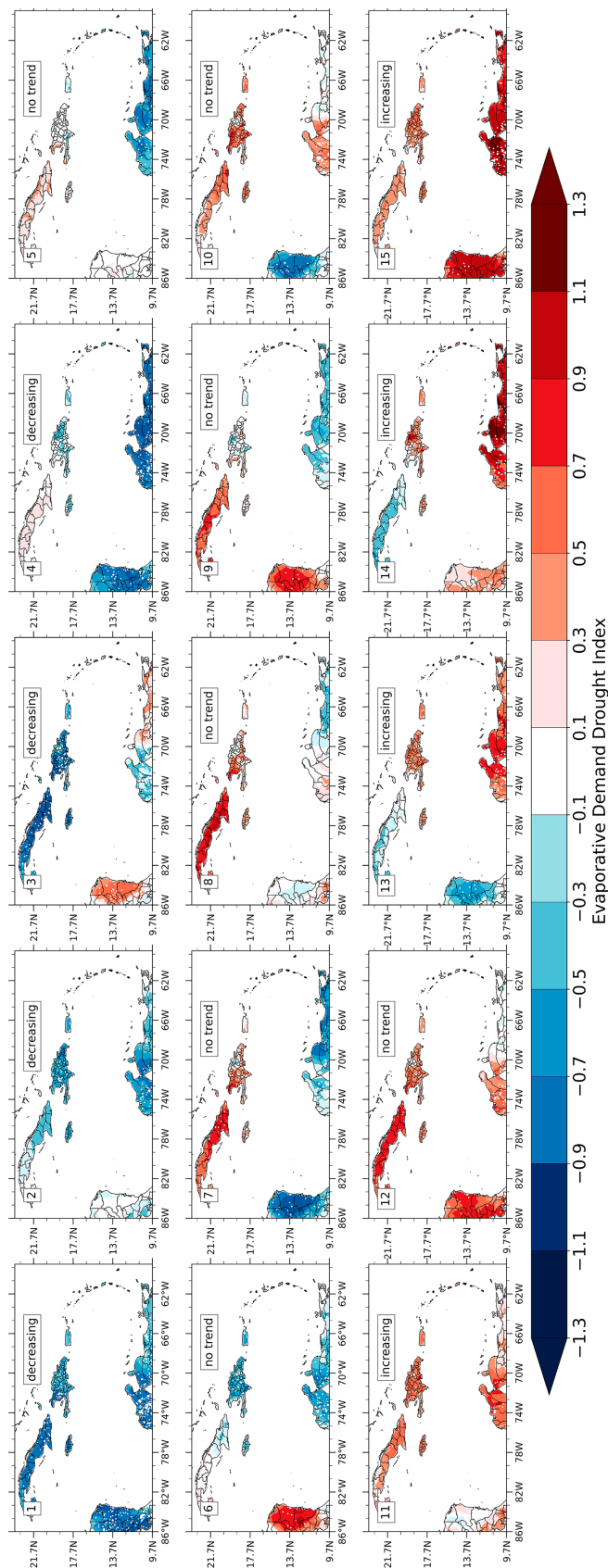


FIG. 2. SOM of EDDI highlighting the most common spatial patterns of EDDI across the Caribbean region. The text in the top right of each panel indicates statistically significant trends (or no trend) in the historical frequencies of the nodes.

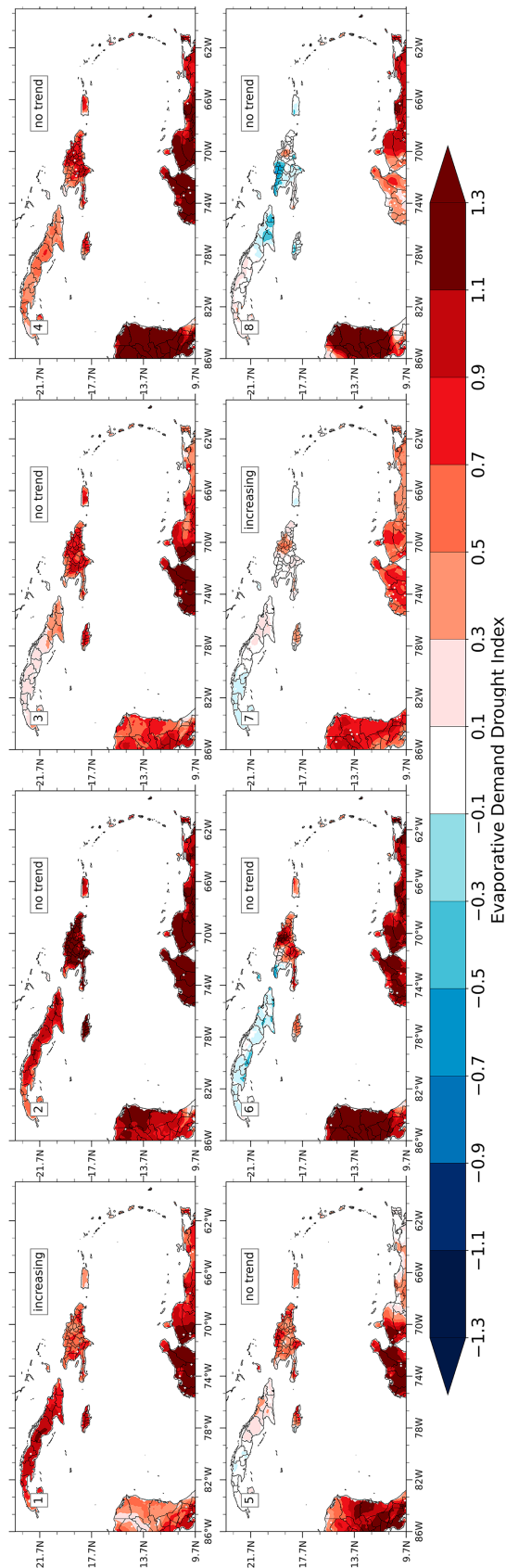


FIG. 3. Nested SOM from the pentads mapping to node 15 in Fig. 2.

clear from Fig. 5 that communities in the Caribbean should be prepared for flash droughts outside of what is colloquially considered the wet season.

c. Intra-Caribbean flash drought modes

The EDDI patterns in Fig. 2 reveal a spatial cohesion to areas experiencing coincident evaporative demand increases. While Fig. 2 is generated from EDDI across all days, intra-Caribbean hotspots of high EDDI may be associated with regional flash drought outbreaks. Figure 6 shows a 2×3 SOM initialized among the large flash droughts in the dataset. A 125-gridpoint minimum size was instituted to ensure that the flash drought was a regionally impactful “outbreak,” rather than a locally isolated event.

The SOM resolved six typologies of flash drought (Fig. 6). Five of the six nodes produce spatially contiguous flash droughts. The SOM identifies flash droughts in Central America (nodes 4–6), Venezuela and Columbia (nodes 3 and 5), Cuba (nodes 2 and 6), and Jamaica, Dominican Republic, and Puerto Rico (node 1). Node 3 showed the most spatially disparate pattern while node 2 exhibited the most spatially contained flash drought type. Figure 6 reinforces the conclusions from Fig. 2, whereby EDDI (Fig. 2) and flash drought (Fig. 6) both demonstrate significant within-basin variability. Consequently, it is clear that the term “Caribbean drought” can be misleading because, at least in the case of flash drought, the drying is concentrated subregionally. For instance, flash drought outbreaks in Puerto Rico commonly occurred with the rest of the Greater Antilles were also experiencing flash drought and did not regularly align with concurrent flash drought in the Central American Caribbean.

d. MJO evolution during Caribbean flash drought

Because of the subseasonal time scale of flash drought onset, as well as the regionalized responses in Fig. 6, the MJO is explored to determine if the SOM nodes have coherent MJO evolutions associated with the flash drought initiation, as well as its adjoining preinitiation and post-initiation periods. The flash droughts were filtered to only include those that occurred with a mean MJO amplitude ≥ 1 across the 25-day flash drought evolution. To test whether the distribution of MJO phase frequency for each flash drought type is random, a chi-square test was deployed.

Figure 7 summarizes the results of the MJO analysis, where the MJO frequency distributions of all six flash drought types from Fig. 6 along with p values from the chi-square tests on the frequency distributions. This test is to provide a statistical analysis of the MJO phase distributions to help to determine if the MJO phase evolutions are equally distributed, and moreover, determine if the distributions illustrated in Fig. 7 are disproportionate at a statistically significant level. If this null hypothesis is rejected (e.g., $p < 0.05$), it would suggest that the MJO phase frequency distributions cannot be ruled out as having some explanatory validity with Caribbean flash drought. This analysis does not, however, allow for the conclusion that MJO causes flash drought, rather, that the MJO

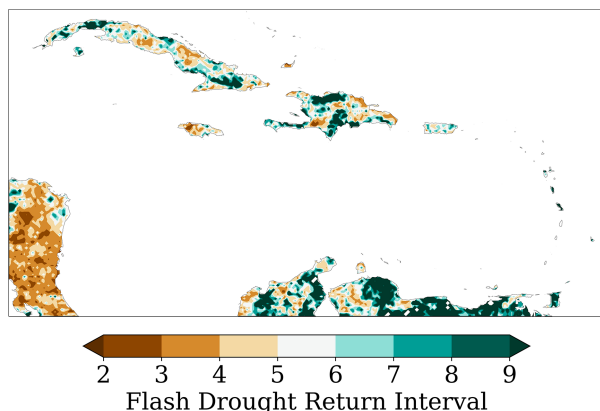


FIG. 4. Caribbean flash drought return interval (yr), 1981–2020.

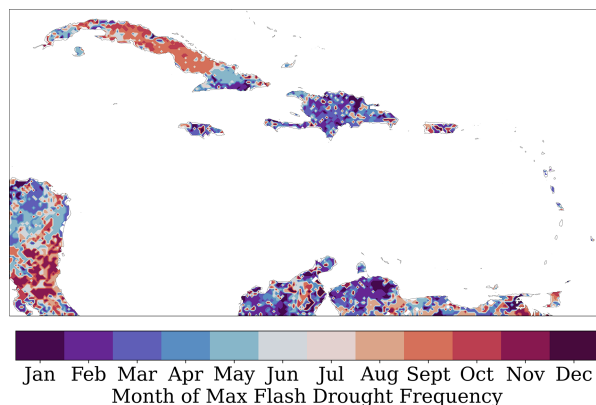


FIG. 5. Month of maximum Caribbean flash drought frequency.

frequency distribution is not equally distributed during flash droughts in the Caribbean.

Each node (i.e., flash drought type) exhibits some statistically significant MJO frequency distributions during at least one of the three stages analyzed. Node 3 exhibits the most equally distributed MJO phase distributions, likely due to that flash-drought type being the least spatially coherent (Fig. 6), while node 5 is fairly even distribution during the initiation stage. In general, the bottom-row of Figs. 6 and 7 represents flash droughts occurring over the Central American Caribbean and these distributions share some similarities in the preceding periods of flash drought where the largest frequencies tend to occur during MJO phases 1 and 8. The preferential MJO phases during the initiation pentad tend to diverge, but phase 2 is among the most frequent initiation MJO phases for four of the six nodes (1, 3, 5, and 6). The results from node 6 suggest that there is an MJO phase envelope change from phase 1 to 2 during the preceding period to the initiation period, respectively. During the drought maintenance period, the MJO phase 2 is preferential for nodes 4 and 6, which both represent forms of flash drought in the Central American coastal plain. peak in the 2–4 phases. Meanwhile, node 5 exhibits a significant preference for MJO phase 4 during the drought maintenance phase.

Node 1, which represents the large flash droughts that initiate in Jamaica, Hispaniola, and Puerto Rico, suggests a range of MJO phases that may be encountered in the preceding period of a flash drought, with MJO phases 4–6 tend to be the least preferred. However, there is a much stronger preference in the initiation phase with MJO phases 2–4 dominating the distribution and phases 7, 8, and 1 occurring infrequently. This is similar to the drought maintenance distribution, where MJO phases 3 and 4 dominate the distribution. Node 2, predominantly flash drought over Cuba, was the most spatially coherent flash drought node in the study. It also exhibited the lowest p values across all three temporal periods. The initiation period shows a strong preference for occurring during phases 3–5 and little preference outside of those phases while drought maintenance period is concentrated in MJO phase 5.

This potential MJO-flash drought mechanism is elucidated by the pan-Caribbean daily precipitation anomalies associated with each node (Fig. 8). Phases 8, 1, and 2 are abnormally wet while Phases 3 and 4 are drier than average. Phases 5, 6, and 7 contain intra-basin variability in precipitation anomaly, so the ramification for flash drought will vary by location. The relationship between the MJO precipitation anomaly and flash drought initiation will be discussed in section 4.

4. Discussion

The findings in this study suggest that the experimental EDDI-based flash drought definition proposed by Pendergrass et al. (2020) can plausibly detect flash drought in tropical climate regimes, particularly in the Caribbean. Our results indicate that not only do flash droughts occur in the Caribbean, but flash droughts are routinely recorded in the 40-yr climatology constructed here. Most of the study domain has a flash drought return interval of 2–5 years (Fig. 4). Additionally, there are indications that flash drought can occur outside of the traditional dry seasons within the Caribbean (Fig. 5).

While many flash droughts identified by the detection criteria used in this study were localized, there were several that initiated simultaneously across a large spatial domain (e.g., >125 ERA5-Land grid points). These high-impact flash droughts tend to occur in discrete clusters in the Caribbean, as evidenced by the SOM in Fig. 6. However, this requirement may also depress occurrences of flash drought in the Windward Islands, whose entire island may be represented by a single grid point. In such cases, for flash droughts in these locations to be detected, they needed to be accompanied by larger flash drought onsets elsewhere in the domain.

Clear associations between MJO phase and flash drought initiation and maintenance are also documented. Somewhat counterintuitively, several flash drought typologies (Fig. 6) initiated during a Caribbean-wide wet MJO phase (Figs. 7 and 8). While this may appear erroneous at first inspection, it instead highlights the value of the EDDI-based flash drought definition in the tropics. For instance, Fig. 1 illustrates how the EDDI identifies a rapid increase in evaporative demand while soil moisture is still increasing from the last pluvial episode. By the

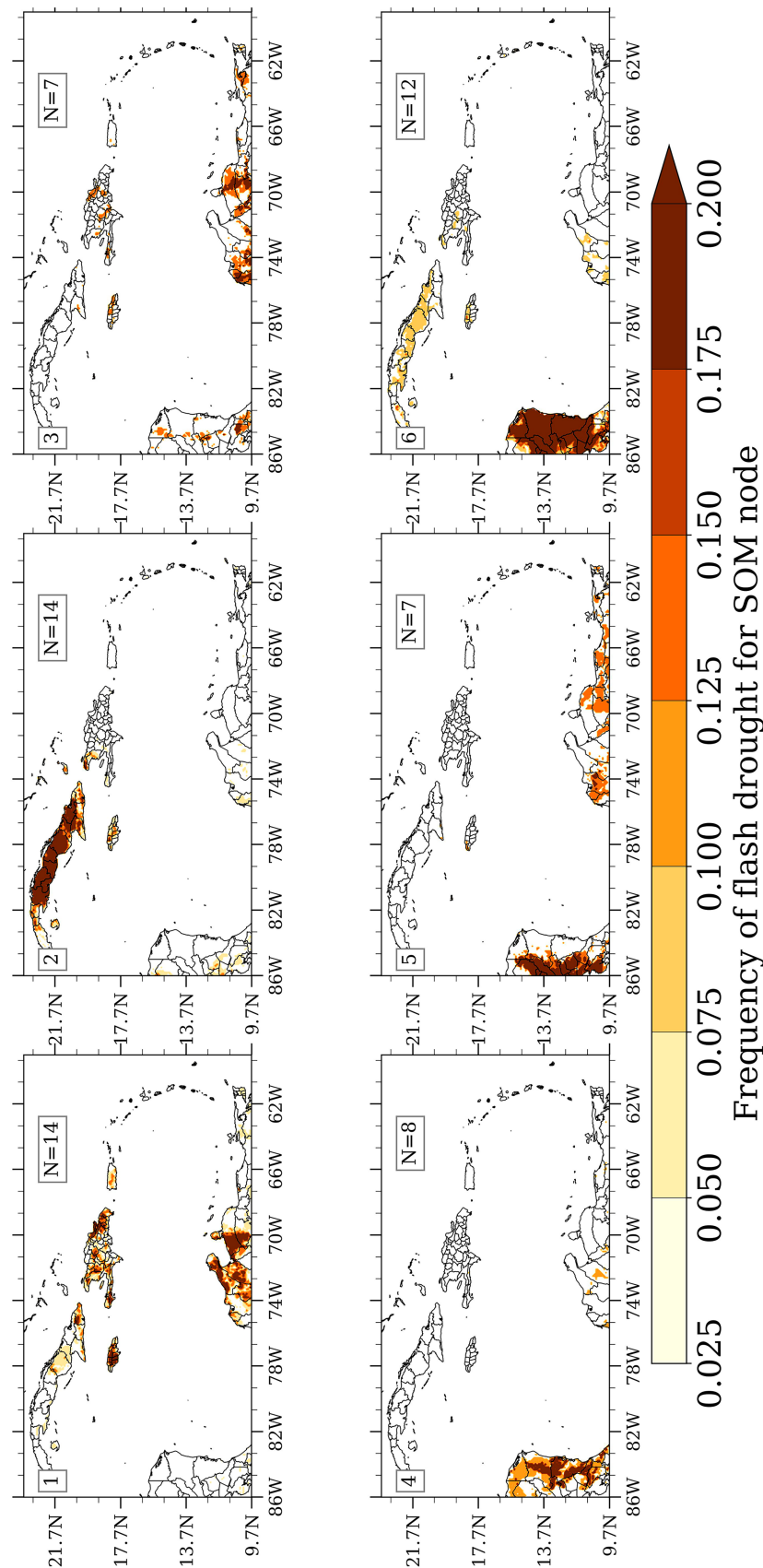


FIG. 6. SOM of large flash drought events (>125 grid points). Contours represent the frequency of flash drought per grid point for each flash drought type.

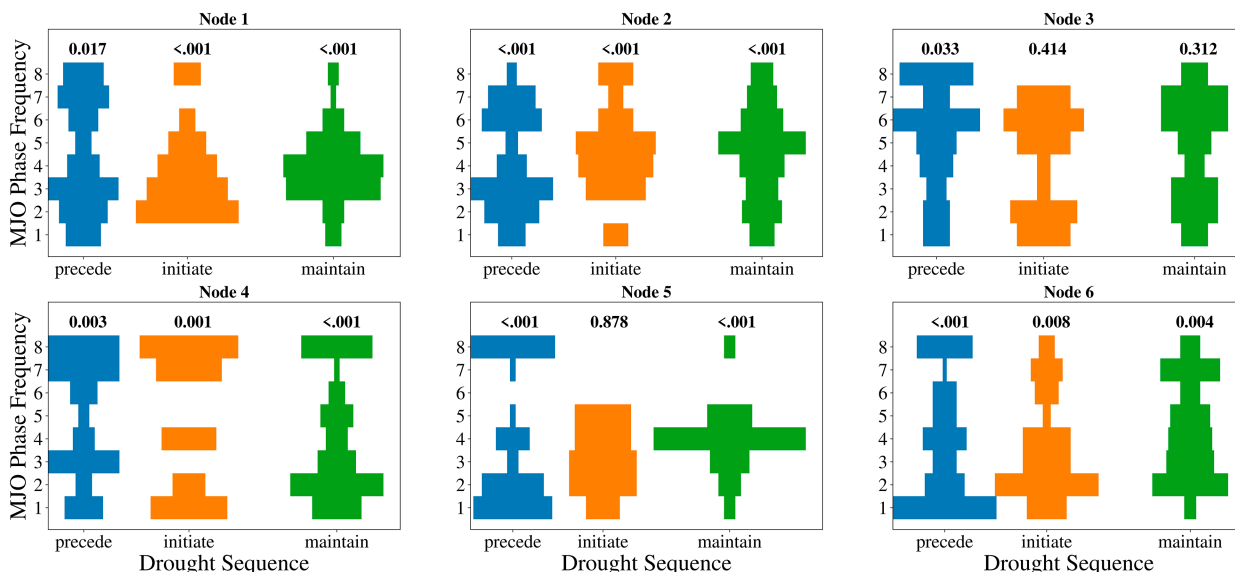


FIG. 7. The distribution of MJO frequencies during the preceding 10 days of a flash drought initiation, the 5 days during a flash drought initiating pentad, and the following 10 day drought maintenance period. The width of each bar indicates the relative frequency of that MJO phase during each period, for each flash drought node from Fig. 6. The chi-square p values are appended to the top of each distribution.

time soil moisture even begins to decrease in response to heightened evaporative demand, forcing actual evapotranspiration higher and drying out the surface, the EDDI has already flagged a flash drought initiation in progress. This same idea is supported by the analysis in Figs. 7 and 8, which shows that flash droughts in the Caribbean are regularly initiated during moist conditions (e.g., MJO phases 1, 2, and 8), rather than exclusively during dry phases as might be assumed. Because the EDDI is formulated to detect increased evaporative demand, rather than precipitation or soil moisture anomalies, it has already been noted an initiating flash drought before the arrival of an MJO dry phase. At that point, the dry phase(s) are only responsible

for maintaining the drought that was already signaled during the antecedent wet phase(s). Though precipitation may be abundant during the MJO wet phase accompanying the flash drought initiation, the EDDI identifies an increase in evaporative demand in the midst of these circumstances.

The flash drought-MJO phase trajectories and their association to basin-wide precipitation demonstrate: 1) the transferability of the EDDI and its flash drought definition to a tropical environment; and 2) the value of the EDDI as an early warning flash drought tool. Even in this wet tropical setting, the EDDI effectively identifies the hydrometeorological regime shifts that will rapidly desiccate the landscape. In fact, the EDDI is able

MJO Daily Precipitation Anomaly

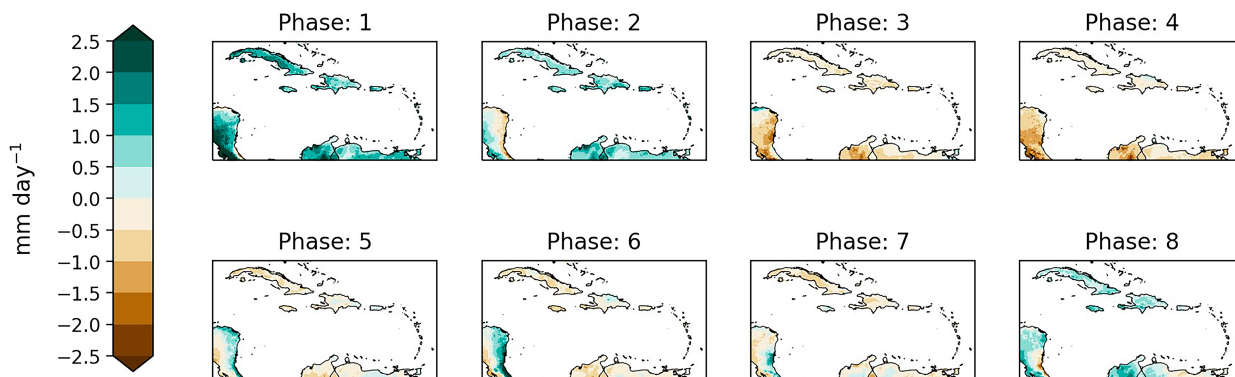


FIG. 8. Daily precipitation anomaly during each MJO phase between 1981 and 2020 according to CHIRPS2. Only days with an MJO amplitude of ≥ 1 were included (8998 days; 61.6%).

to identify the onset of flash drought even on the heels of the last pluvial episode (Figs. 1 and 8), similar to the findings of Mukherjee and Mishra (2022), and capture the rapid regime shift that is soon to occur. Because flash droughts' greatest danger arises from their rapid and unexpected development (often during periods when drought seemed quite unlikely even a couple weeks earlier), the EDDI is shown to be an effective front-line warning tool for signaling the imminent arrival of water stress, even in the absence of soil-moisture monitoring stations. Such an aptitude is particularly valuable in the Caribbean where limited groundwater and surface water reservoirs offer little, if any, protection from periods of drought.

5. Conclusions

While numerous studies have examined the flash drought paradigm across a wide range of midlatitude settings (e.g., Mo and Lettenmaier 2016; Otkin et al. 2018), the transferability of flash drought to the world's tropics has been relatively unexplored. Because the cadence of precipitation in moist tropical regions differs substantially from the midlatitude testbeds where flash drought has received the most attention (Table 1), there remains a need to critically examine the suitability of midlatitude-centric flash drought criteria to tropical environments. Consequently, this study tested the flash drought definition proposed by Pendergrass et al. (2020), which is predicated on the evaporative demand drought index (Hobbins et al. 2016), over the Caribbean basin.

The EDDI revealed regionally coherent patterns of evaporative stress (Fig. 2), and when compared with the Pendergrass flash drought definition, 46 instances of expansive flash drought events were identified within the Caribbean (Fig. 6). The distribution of these flash droughts across the basin revealed high intra-regional variability such that the term "Caribbean drought" loses most meaning. While flash drought was not uncommon in this tropical region, it was often concentrated over specific subregions, such as northern South America, the Central American Caribbean, the Greater Antilles, etc. In fact, the largest flash drought that was identified within the EDDI dataset initiated during the 5–9 June 2015 pentad when 1394 grid points (approximately 110 000 km²), corresponding to 32% of the study area, initiated a flash drought sequence. This temporally aligns with one of the highest magnitude long-term droughts in the last 40 years in parts of the Caribbean (Mote et al. 2017). This highlights that even in its most expansive form, Caribbean drought is not a monolithic concept.

Meanwhile, frequent instances of isolated, transient flash droughts were rampant within the EDDI analysis, but it was unclear whether these "flash droughts" were physically meaningful events. However, because flash drought occurring on small volcanic islands in the eastern Caribbean (e.g., Martinique) is necessarily small and isolated, it is possible that legitimate eastern Caribbean flash droughts were filtered out in order to analyze more expansive, regionally impactful flash droughts within the basin. Future research should examine these flash droughts in more detail, examine the precise sequences of leads and lags in surface hydrological parameters (e.g., Mukherjee and Mishra 2022), and link them to MJO

phases as was done for larger flash drought "outbreaks." Because these smaller Caribbean landscapes are perhaps the most water-vulnerable locations in the entire basin, the extension of MJO-based flash drought prediction to these islands is particularly valuable.

While flash droughts are challenging to predict by virtue of their rapid onset, the statistically significant associations between regional flash drought configurations and MJO phase suggests some degree of subseasonal predictability. Additional research should examine the mechanisms underlying the flash drought-MJO connections. For instance, are these MJO phases related to enhanced Saharan dust advection across the Atlantic, midlevel ridging and surface temperature warm anomalies, or a reduction in tropical waves that would otherwise generate precipitation? As the physical mechanisms supporting the MJO's influence on Caribbean flash drought are made clearer, its role as a subseasonal flash drought predictor can be expanded.

Beyond prediction, the prevalence of tropical flash drought in the Caribbean shown here necessitates future work in examining the agricultural and ecological impacts of the rapid drying events. For instance, in Puerto Rico and the U.S. Virgin Islands, crop insurance policies may be tied to the drought category (if any) resolved by the U.S. Drought Monitor (Mercado-Díaz et al. 2023). However, this instrument may be slow to recognize the emergence of a flash drought event, placing the Puerto Rican agricultural industry in a difficult position. Given the regularity of flash drought across the Caribbean, future work should seek to understand the extent to which flash droughts are associated with tangible economic losses, and by extension, how these events should be monitored and communicated to stakeholders in a timely fashion.

Acknowledgments. This work was supported by the NOAA Modeling Analysis and Prediction Program (MAPP) under Award NA20OAR4310416. The authors also acknowledge the helpful feedback from two anonymous reviewers.

Data availability statement. Datasets created during this study are available in the Virginia Tech University Libraries Data Repository (<https://doi.org/10.7294/21543108>). These datasets were derived from the following public domain resource: ERA5-Land reanalysis (<https://www.ecmwf.int/en/era5-land>).

REFERENCES

- Allen, R. G., L. S. Pereira, D. Raes, and M. Smith, 1998: Crop evapotranspiration—Guidelines for computing crop water requirements. FAO Irrigation and Drainage Paper 56, 300 pp., www.fao.org/docrep/X0490E/X0490E00.htm.
- , I. A. Walter, R. Elliot, T. Howell, D. Itenfisu, and M. Jensen, 2005: The ASCE standardized reference evapotranspiration equation. ASCE-EWRI Task Committee Rep., 70 pp., <https://epic.awi.de/id/eprint/42362/1/ascestzdetmain2005.pdf>.
- Beguieria, S., S. M. Vicente-Serrano, F. Reig, and B. Latorre, 2014: Standardized precipitation evapotranspiration index (SPEI) revisited: Parameter fitting, evapotranspiration models,

- tools, datasets and drought monitoring. *Int. J. Climatol.*, **34**, 3001–3023, <https://doi.org/10.1002/joc.3887>.
- Cassano, E. N., J. M. Glisan, J. J. Cassano, W. J. Gutowski Jr., and M. W. Seefeldt, 2015: Self-organizing map analysis of widespread temperature extremes in Alaska and Canada. *Climate Res.*, **62**, 199–218, <https://doi.org/10.3354/cr01274>.
- Debbage, N., P. Miller, S. Poore, K. Morano, T. Mote, and J. M. Shepherd, 2017: A climatology of atmospheric river interactions with the southeastern United States coastline. *Int. J. Climatol.*, **37**, 4077–4091, <https://doi.org/10.1002/joc.5000>.
- Ford, T. W., and C. F. Labosier, 2017: Meteorological conditions associated with the onset of flash drought in the eastern United States. *Agric. For. Meteorol.*, **247**, 414–423, <https://doi.org/10.1016/j.agrformet.2017.08.031>.
- Funk, C., and Coauthors, 2015: The climate hazards infrared precipitation with stations—A new environmental record for monitoring extremes. *Sci. Data*, **2**, 150066, <https://doi.org/10.1038/sdata.2015.66>.
- Gingrich, T. M., 2022: Synoptic-scale atmospheric conditions associated with flash drought initiation in Puerto Rico and the Caribbean. M.S. thesis, Dept. of Geography, Virginia Tech, 207 pp., <https://vtechworks.lib.vt.edu/handle/10919/110352>.
- Hersbach, H., and Coauthors, 2020: The ERA5 global reanalysis. *Quart. J. Roy. Meteor. Soc.*, **146**, 1999–2049, <https://doi.org/10.1002/qj.3803>.
- Hewitson, B. C., and R. G. Crane, 2002: Self-organizing maps: Applications to synoptic climatology. *Climate Res.*, **22**, 13–26, <https://doi.org/10.3354/cr022013>.
- Hobbins, M. T., A. Wood, D. J. McEvoy, J. L. Huntington, C. Morton, M. Anderson, and C. Hain, 2016: The evaporative demand drought index. Part I: Linking drought evolution to variations in evaporative demand. *J. Hydrometeorol.*, **17**, 1745–1761, <https://doi.org/10.1175/JHM-D-15-0121.1>.
- Jensen, M. E., R. D. Burman, R. G. Allen, and American Society of Civil Engineers, Eds., 1990: *Evapotranspiration and Irrigation Water Requirements: A Manual*. The Society, 332 pp.
- Köhler, L., C. Tobón, K. F. A. Frumau, and L. A. (Sampurno) Bruijnzeel, 2007: Biomass and water storage dynamics of epiphytes in old-growth and secondary montane cloud forest stands in Costa Rica. *Plant Ecol.*, **193**, 171–184, <https://doi.org/10.1007/s11258-006-9256-7>.
- Madden, R. A., and P. R. Julian, 1972: Description of global-scale circulation cells in the tropics with a 40–50 day period. *J. Atmos. Sci.*, **29**, 1109–1123, [https://doi.org/10.1175/1520-0469\(1972\)029<1109:DOGSCC>2.0.CO;2](https://doi.org/10.1175/1520-0469(1972)029<1109:DOGSCC>2.0.CO;2).
- , and —, 1994: Observations of the 40–50-day tropical oscillation—A review. *Mon. Wea. Rev.*, **122**, 814–837, [https://doi.org/10.1175/1520-0493\(1994\)122<0814:OOTDTC>2.0.CO;2](https://doi.org/10.1175/1520-0493(1994)122<0814:OOTDTC>2.0.CO;2).
- Malardel, S., N. Wedi, W. Deconinck, M. Diamantakis, C. Kuehnlein, G. Mozdynski, M. Hamrud, and P. Smolarkiewicz, 2016: A new grid for the IFS. *ECMWF Newsletter*, No. 146, ECMWF, Reading, United Kingdom, 23–28, <https://doi.org/10.21957/zwdu9u5i>.
- Mattingly, K. S., C. A. Ramseyer, J. J. Rosen, T. L. Mote, and R. Muthyala, 2016: Increasing water vapor transport to the Greenland Ice Sheet revealed using self-organizing maps. *Geophys. Res. Lett.*, **43**, 9250–9258, <https://doi.org/10.1002/2016GL070424>.
- McKee, T. B., N. J. Doesken, and J. Kleist, 1993: The relationship of drought frequency and duration to time scales. *Proc. Eighth Conf. on Applied Climatology*, Anaheim, CA, Amer. Meteor. Soc., 179–183.
- Mercado-Díaz, J. A., E. Holupchinski, N. Álvarez-Berrios, W. A. Gould, P. Miller, T. Mote, C. Ramseyer, and G. González, 2023: Fostering knowledge-exchange and collaboration among drought-related initiatives in the Caribbean. *Bull. Amer. Meteor. Soc.*, **104**, E1146–E1153, <https://doi.org/10.1175/BAMS-D-23-0054.1>.
- Miller, P. W., T. L. Mote, C. A. Ramseyer, A. E. Van Beusekom, M. Scholl, and G. González, 2018: A 42 year inference of cloud base height trends in the Luquillo mountains of north-eastern Puerto Rico. *Climate Res.*, **76**, 87–94, <https://doi.org/10.3354/cr01529>.
- , —, and —, 2019: An empirical study of the relationship between seasonal precipitation and thermodynamic environment in Puerto Rico. *Wea. Forecasting*, **34**, 277–288, <https://doi.org/10.1175/WAF-D-18-0127.1>.
- Mo, K. C., and D. P. Lettenmaier, 2015: Heat wave flash droughts in decline. *Geophys. Res. Lett.*, **42**, 2823–2829, <https://doi.org/10.1002/2015GL064018>.
- , and —, 2016: Precipitation deficit flash droughts over the United States. *J. Hydrometeorol.*, **17**, 1169–1184, <https://doi.org/10.1175/JHM-D-15-0158.1>.
- Mote, T. L., C. A. Ramseyer, and P. W. Miller, 2017: The Saharan air layer as an early rainfall season suppressant in the eastern Caribbean: The 2015 Puerto Rico drought. *J. Geophys. Res. Atmos.*, **122**, 10 966–10 982, <https://doi.org/10.1002/2017JD026911>.
- Mukherjee, S., and A. K. Mishra, 2022: Global flash drought analysis: Uncertainties from indicators and datasets. *Earth's Future*, **10**, e2022EF002660, <https://doi.org/10.1029/2022EF002660>.
- Muñoz-Sabater, J., and Coauthors, 2021: ERA5-Land: A state-of-the-art global reanalysis dataset for land applications. *Earth Syst. Sci. Data*, **13**, 4349–4383, <https://doi.org/10.5194/essd-13-4349-2021>.
- O’Connell, C. S., L. Ruan, and W. L. Silver, 2018: Drought drives rapid shifts in tropical rainforest soil biogeochemistry and greenhouse gas emissions. *Nat. Commun.*, **9**, 1348, <https://doi.org/10.1038/s41467-018-03352-3>.
- Osman, M., B. F. Zaitchik, H. S. Badr, J. I. Christian, T. Tadesse, J. A. Otkin, and M. C. Anderson, 2021: Flash drought onset over the contiguous United States: Sensitivity of inventories and trends to quantitative definitions. *Hydrol. Earth Syst. Sci.*, **25**, 565–581, <https://doi.org/10.5194/hess-25-565-2021>.
- Otkin, J. A., M. Svoboda, E. D. Hunt, T. W. Ford, M. C. Anderson, C. Hain, and J. B. Basara, 2018: Flash droughts: A review and assessment of the challenges imposed by rapid-onset droughts in the United States. *Bull. Amer. Meteor. Soc.*, **99**, 911–919, <https://doi.org/10.1175/BAMS-D-17-0149.1>.
- Pendergrass, A. G., and Coauthors, 2020: Flash droughts present a new challenge for subseasonal-to-seasonal prediction. *Nat. Climate Change*, **10**, 191–199, <https://doi.org/10.1038/s41558-020-0709-0>.
- Ramseyer, C. A., and T. L. Mote, 2016: Atmospheric controls on Puerto Rico precipitation using artificial neural networks. *Climate Dyn.*, **47**, 2515–2526, <https://doi.org/10.1007/s00382-016-2980-3>.
- , and —, 2018: Analysing regional climate forcing on historical precipitation variability in northeast Puerto Rico. *Int. J. Climatol.*, **38**, e224–e236, <https://doi.org/10.1002/joc.5364>.
- , and N. Teale, 2021: On the emerging global relevance of atmospheric rivers and impacts on landscapes and water resources. *Prog. Phys. Geogr.*, **45**, 965–978, <https://doi.org/10.1177/03091333211058893>.
- , P. W. Miller, and T. L. Mote, 2019: Future precipitation variability during the early rainfall season in the El Yunque

- National Forest. *Sci. Total Environ.*, **661**, 326–336, <https://doi.org/10.1016/j.scitotenv.2019.01.167>.
- , and Coauthors, 2022: Identifying eastern U.S. atmospheric river types and evaluating historical trends. *J. Geophys. Res. Atmos.*, **127**, e2021JD036198, <https://doi.org/10.1029/2021JD036198>.
- Sheridan, S. C., and C. C. Lee, 2011: The self-organizing map in synoptic climatological research. *Prog. Phys. Geogr.*, **35**, 109–119, <https://doi.org/10.1177/0309133310397582>.
- Teale, N., and D. A. Robinson, 2020: Patterns of water vapor transport in the eastern United States. *J. Hydrometeor.*, **21**, 2123–2138, <https://doi.org/10.1175/JHM-D-19-0267.1>.
- Vesanto, J., J. Himberg, E. Alhoniemi, and J. Parhankangas, 2000: SOM toolbox for Matlab 5. Rep. A57, 60 pp., <http://www.cis.hut.fi/projects/somtoolbox/package/papers/techrep.pdf>.
- Vicente-Serrano, S. M., S. Beguería, and J. I. López-Moreno, 2010: A multiscalar drought index sensitive to global warming: The standardized precipitation evapotranspiration index. *J. Climate*, **23**, 1696–1718, <https://doi.org/10.1175/2009JCLI2909.1>.
- Wheeler, M. C., and H. H. Hendon, 2004: An all-season real-time multivariate MJO index: Development of an index for monitoring and prediction. *Mon. Wea. Rev.*, **132**, 1917–1932, [https://doi.org/10.1175/1520-0493\(2004\)132<1917:AARMMI>2.0.CO;2](https://doi.org/10.1175/1520-0493(2004)132<1917:AARMMI>2.0.CO;2).
- Wilks, D. S., 2011: *Statistical Methods in the Atmospheric Sciences*. 3rd ed. International Geophysics Series, Vol. 100, Academic Press, 704 pp.
- Yuan, X., L. Wang, P. Wu, P. Ji, J. Sheffield, and M. Zhang, 2019: Anthropogenic shift towards higher risk of flash drought over China. *Nat. Commun.*, **10**, 4661, <https://doi.org/10.1038/s41467-019-12692-7>.
- Zhang, C., 2005: Madden-Julian Oscillation. *Rev. Geophys.*, **43**, RG2003, <https://doi.org/10.1029/2004RG000158>.
- Zimmerman, J. K., J. A. Hogan, S. Rifkin, and S. Stankavitch, 2016: Responses of forest vegetation to unusual drought in wet forest in eastern Puerto Rico: A “dry run” for climate change? *2016 Fall Meeting*, San Francisco, CA, Amer. Geophys. Union, Abstract B42A-05.